Vol. **113** (2008) *ACTA PHYSICA POLONICA A* No. 5

Proceedings of the 37th Polish Seminar on Positron Annihilation, Lądek-Zdrój 2007

Simulation of Positron Annihilation Response to Mechanical Deformation of Nanostructured AgCo

O. Melikhova[a,b], J. Kuriplach[a], J. Čížek[a], I. Procházka[a], M. Hou[b], S. Pisov[b,c] and E. Zhurkin[b,d]

[a]Department of Low Temperature Physics, Faculty of Mathematics and Physics
Charles University in Prague
V Holesovickach 2, CZ-180 00 Prague 8, Czech Republic
[b]Physique des Solides Irradiés et des Nanostructures CP234
Université Libre de Bruxelles, Bd du Triomphe, B-1050 Brussels, Belgium
[c]Faculty of Physics, University of Sofia
5 James Bourchier str., 1164 Sofia, Bulgaria
[d]Department of Experimental Nuclear Physics, Physical & Mechanical Faculty
K-89, St. Petersburg State Polytechnical University
29 Polytekhnicheskaya str., 195251 St. Petersburg, Russia

Nanostructured materials attract nowadays a broad attention due to their specific properties. Defects play an essential role in material properties so their characterisation is very important. The evolution of the various open volume defects in AgCo nanowire modelled samples obtained using molecular dynamics was studied. Isothermal and isoenergetic deformation mechanisms are considered. General analyses of open volume defects concerning their size and their chemical environment were performed. Positron lifetimes, binding energies, and high momentum parts of the momentum distribution of annihilation γ-quanta were calculated for selected defects.

PACS numbers: 78.70.Bj, 71.15.Pd, 61.46.Hk

1. Introduction

Nowadays, there is a fast growing interest in the synthesis as well as in the mechanical testing of nanostructural materials. Some of them are made of clusters with compositions that do not exist at the macroscopic scale. Silver and cobalt are immiscible elements and AgCo nanostructured materials consist of rather well separated Ag and Co phases. The spatial arrangement of Ag and Co atoms in clusters may consist in a Co core surrounded by an Ag shell. The Ag shell is not crystalline, but it displays a layered structure induced by crystalline Co cores [1].

Since Ag shells are noncrystalline, they are easily deformed, which results in the superplastic behaviour predicted for AgCo cluster assembled materials (CAM) [1]. Possible thickness of this noncrystalline shell was predicted to increase with temperature. Its structure is not altered by mechanical deformation and Ag behaves as an ordinary viscous fluid carrying solid Co grains. In this case only the mechanically induced coalescence of Co clusters is expected as a limiting factor to the superplastic behaviour of AgCo CAM [1].

Positrons are sensitive to free volumes (FVs) in the studied material which are present within noncrystalline Ag shells as well as at the Ag/Co interface. The possibility to resolve different types of defects in AgCo nanostructured materials and to follow their evolution during deformation experimentally by means of positron annihilation spectroscopy is examined in the present work.

2. Samples

Nanostructured AgCo nanowire modelled by molecular dynamics (MD) was chosen for investigation. The cohesion of the immiscible AgCo system is modelled by an embedded atom model [2] with functionals given in Ref. [3]. The associated equilibrium lattice constant was $a = 4.09$ Å at 0 K. Crystalline Co grains were embedded into an Ag crystalline cylinder with its axis along the [001] direction and with an initial diameter of 10 nm and then the whole system was set to relax by MD at 300 K. The Ag crystal structure turned out to be unstable and transformed into the same layered structure as predicted in AgCo nanoclusters and AgCo CAM [1]. Deformation was modelled by changing the length of the nanowire in the axial direction and a periodic boundary condition was applied in order to model a cylindrical wire with an infinite length. Both isothermal (300 K) and isoenergetic deformation mechanisms are considered, the latter one reflects the condition for the mechanical work to fully convert into heat during deformation. The evolution of the sample with strain $\varepsilon_{zz} = (l - l_0)/l_0$, where l_0 and l are the lengths of the sample before and after deformation, respectively, was followed by deformation steps $\Delta\varepsilon_{zz} = 0.05$ until $\varepsilon_{zz} = 1.00$. The detailed description of the sample preparation procedure and deformation experiment can be found in Ref. [4].

3. Computational analysis methods

Analyses of FVs were made by means of the FREEVOL programme [5]. Parameters' setting in FREEVOL was done in order to allow detecting open volumes of about 5.5 Å^3 (≈ 0.3 of Ag single vacancy size) and larger. The chemical enviroment of defects was determined by counting atoms with positions that do not exceed the distance 2 Å from the defect surface and the chemical fraction N_1/N is the number of Ag atoms divided by the total number of atoms at the nearest neighbourhood of the FV.

Positron lifetimes (PLs) and high momentum parts (HMPs) of the momentum distribution of annihilation γ-quanta were calculated by means of the ATSUP programme [6, 7] based on the atomic superposition method [8, 9]. The enhancement factor and correlation part of the positron potential were determined using the parameterisation obtained by Boroński and Nieminen [10]. HMP calculations were carried out using the computational scheme described in Ref. [11]. Further computational details are specified in Sect. 4.2.

4. Results

4.1. Analyses of FV

Characteristics of FVs found for the sample deformed isothermally and isoenergetically are shown in Fig. 1 for selected extensions. In both cases more than 50% of FVs are rather small, with the size ≈ 5.5 Å^3 (≈ 0.3 Ag vacancy; see Fig.

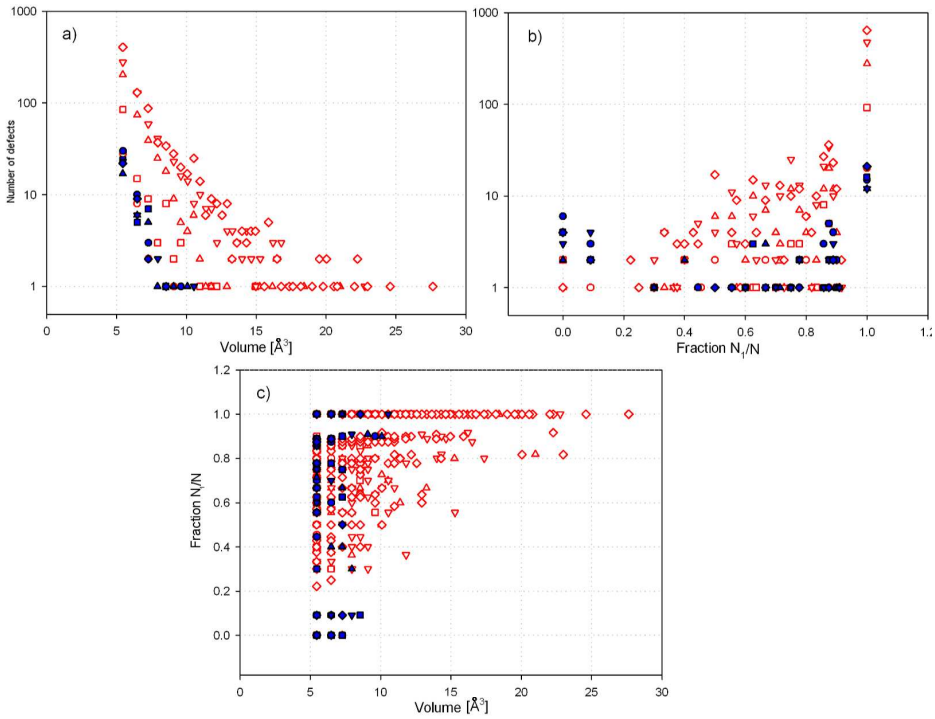

Fig. 1. FV characteristics of the sample deformed isothermally (filled symbols) and isoenergetically (empty symbols): (a) the number of FVs vs. their size, (b) number of FVs vs. the fraction of Ag atoms among the nearest neighbours of the FVs and (c) correlation between chemical environment and FV size are plotted for the strain $\varepsilon_{zz} = 0.00$ (circles), $\varepsilon_{zz} = 0.25$ (squares), $\varepsilon_{zz} = 0.50$ (triangles up), $\varepsilon_{zz} = 0.75$ (triangles down) and $\varepsilon_{zz} = 1.00$ (diamonds).

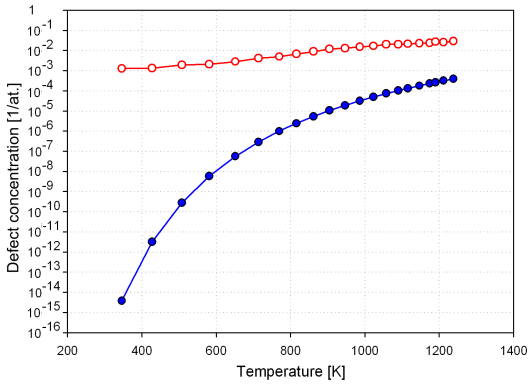

Fig. 2. The evolution of the FV concentration during isoenergetic deformation is shown by empty symbols. The equilibrium vacancy concentration in pure fcc Ag estimated for corresponding temperatures is shown by filled symbols.

1a) and they appear in the pure Ag phase (Fig. 1b). During isothermal deformation, the amount, size, and chemical environment of the FVs show no clear evolution. During isoenergetic deformation both the quantity and the size of the FVs increase. Most of the FVs as well as the FVs with the largest size ($\approx$ 3 Ag vacancy) are located in Ag and the size of FVs as well as their number decrease with the increasing Co content around defects. Some of the FVs found in pure Co before deformation were annealed out with the increasing temperature during deformation. The total volume of defects increases from $\approx$ 250 up to 6550 Å^3 during isoenergetic deformation and it remains approximately constant during isothermal deformation. This means that mechanical strain causes no structural changes in the sample and all changes found are induced by the heat accumulated during isoenergetic deformation. Simultaneously, the increase in the total number of FVs with temperature cannot be explained by an increasing equilibrium vacancy concentration, as shown in Fig. 2.

The equilibrium vacancy concentration C_V in fcc Ag was estimated using the formula

$$C_V = \exp(S_{1V}/k)\exp(-E_{1V}/kT), \tag{1}$$

where $S_{1V} = 2.0k$ [12] is the monovacancy formation entropy, $E_{1V} = 1.05$ eV [13] is the monovacancy formation energy, k is the Boltzmann constant and T is the temperature. Figure 2 shows the temperature dependence of C_V calculated from Eq. (1) and the FV concentration during the isoenergetic deformation. Obviously, FV concentration is much higher than the equilibrium vacancy concentration at all temperatures. Even at the melting point of Ag ($\approx$ 1000 K), C_V is only $\approx$ 0.3% of the FV concentration.

The increase in the FV concentration at moderate temperature ($<$ 1000 K) can be explained by a non-crystalline state of Ag. Indeed, the layered structure of

Ag around Co clusters is highly defective and the energy needed to create defects is thus much lower than for crystalline Ag. It also comes along with the finding that the thickness of the layered structure around Co clusters increases with the increasing temperature for the AgCo CAM [1].

In general, since mechanical strain induced no structural changes in the sample, the superplasticity can be predicted for AgCo nanowires for the same reason as for AgCo CAM [1]. Coalescence of Co clusters, which puts limitation on the superplastic behaviour [1], was observed in the case of AgCo nanowires during isoenergetic deformation [4]. The coalescence started approximately at the strain $\varepsilon_{zz} = 0.45$ and at higher strains a coaxial structure was formed with Co covered by Ag [4]. There is an indication that this process may be connected with the increasing number of defects that appeared on the Ag/Co interface.

4.2. Simulation of positron response

For simulation of positron response, small regions around FVs of different sizes and chemical environment were cut from the virtual AgCo nanowire. Boxes/cuts used for positron calculations have typically the $20 \times 20 \times 20$ Å^3 size and contain ≈ 500 atoms. Because such cuts are not periodic, false open volumes can exist on the box boundary when periodic boundary conditions are applied [6]. In order to avoid positron trapping at these false open volumes, the positron wave function was set to zero at the box boundary. Parameters of FVs for the selected cuts — that represent characteristic cases from the whole sample — and results of calculations are shown in Table.

TABLE

Simulated positron and FV characteristics for the selected defects in the AgCo nanowire. The symbol PBE denotes positron binding energy for the defect, W_1/W is relative contribution of positron annihilations with Ag electrons to the W parameter. A1, A2 and C1, C2 denote defects located in Ag and Co environment, respectively, AC1 denotes defect located at the Ag/Co interface. [a]The whole FV which takes place in positron trapping.

Defect	Volume [Å^3]	Fraction N_1/N	Lifetime [ps]	PBE [eV]	W parameter	W_1/W
A1	7.3	1.0	156	−0.5	0.0171	0.99
A2	31.9	1.0	237	−2.36	0.0153	0.99
C1	6.9	0.0	166	−1.72	0.0320	0.00
C2	6.9 (13.5[a])	0.0	172	−3.27	0.0285	0.13
AC1	7.1	0.5	162	−0.72	0.0203	0.64

As a reference the positron response was calculated also for the bulk material (pure fcc Ag and Co) with and without vacancy clusters. Clusters up to 13 vacancies were created by removing individual atoms from a $4 \times 4 \times 4$ fcc lattice

unit supercell. Lattice constants 4.090 Å and 3.615 Å were used for Ag and Co, respectively. Considering that Co clusters have also the fcc structure (and not hcp as bulk crystalline Co), the Co lattice constant used in calculations was deduced from the pair correlation functions for AgCo nanowire [4]. The positron ground state energies calculated by the ATSUP technique for fcc Ag and Co bulk were $E_{\mathrm{Ag}} = 0.05$ eV and $E_{\mathrm{Co}} = 4.75$ eV, respectively. E_{Ag} was used as a reference to calculate the positron binding energy (PBE) for defects A1 and A2 and vacancy clusters in Ag. In the same way, E_{Co} was used to calculate the PBE for defects C1 and C2 and vacancy clusters in Co. In order to account for the Ag–Co affinity difference, the positron response for AC1 defect was calculated applying a shift (E_{S}) of the positron potential around Co atomic sites in a sphere with the radius $R = 2.75$ Å [7]. An appropriate E_{S} value was estimated using the formula

$$E_{\mathrm{S}} = (E_{\mathrm{Ag}} - E_{\mathrm{Co}}) + (A^{+}_{\mathrm{Co}} - A^{+}_{\mathrm{Ag}}), \tag{2}$$

where $A^{+}_{\mathrm{Ag}} = -5.36$ eV and $A^{+}_{\mathrm{Co}} = -4.18$ eV [14] are the positron affinities of Ag and Co, respectively. The meaning of this formula is that the potential of Co atoms is shifted in order to get the correct positron energy differences between the Ag and the Co phases (see [7] for details). Then, the reference level E_{AgCo} for calculating PBE at AC1 was estimated as

$$E_{\mathrm{AgCo}} = E_{\mathrm{S}} + E_{\mathrm{Ag}} W_1/W + E_{\mathrm{Co}}(1 - W_1/W), \tag{3}$$

where W_1/W is the ratio of the contribution W_1, which comes from annihilation with the Ag core electrons, to the total W. This expression compensates the shift of the potential in the defect and "weights" E_{Ag} and E_{Co} reference levels according

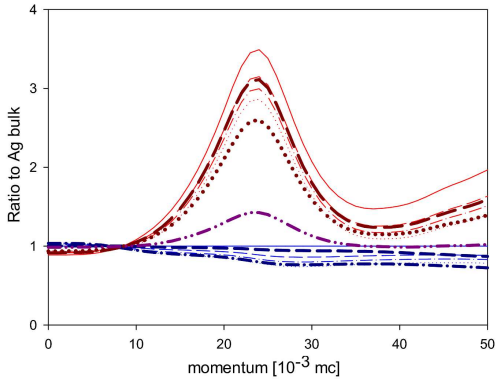

Fig. 3. HMP ratio (related to Ag bulk) for selected defects. The following notation is used in the figure: thin lines represent Ag (lower at high momenta) and Co (upper at high momenta) reference bulk (solid line) and vacancy clusters (monovacancy — medium dash line, di-vacancy — dash-dot line, triple-vacancy — dotted line). Thick lines represent the selected defects in the AgCo nanowire (A1 — medium dash line, A2 — dash-dot line, C1 — long dash line, C2 — dotted line, AC1 — dash-dot-dot line).

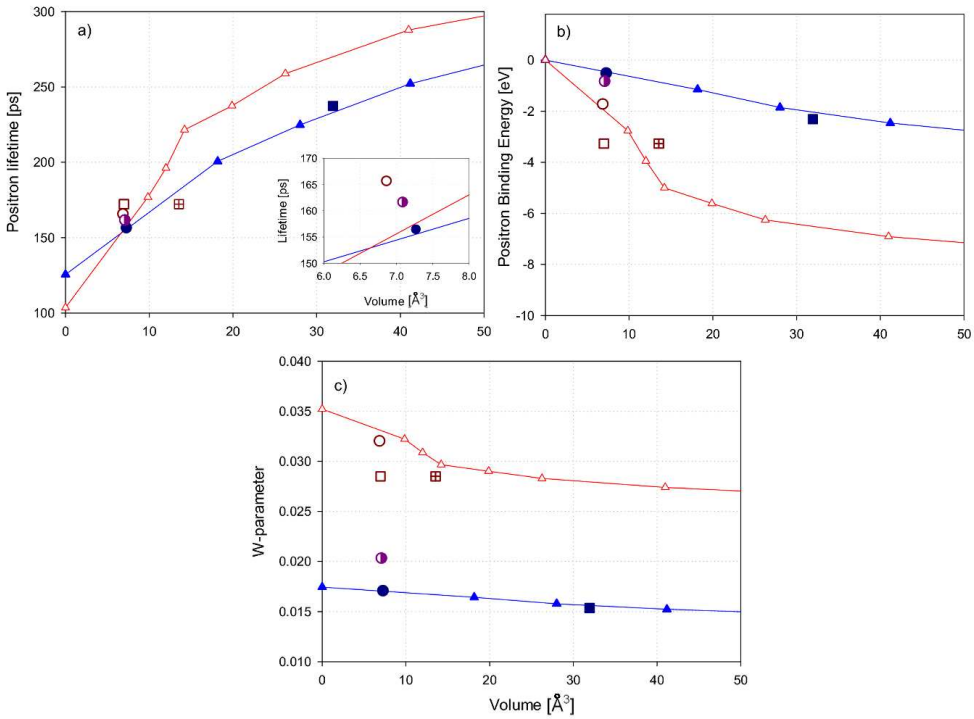

Fig. 4. Positron lifetime (a), positron binding energy (b), and W parameter (c) calculated for the selected defects in the AgCo nanowire (A1 — filled circle; A2 — filled square; C1 — empty circle; C2 — empty and crossed square; AC1 — semi-filled circle). Corresponding reference values calculated for the Ag and Co bulk and vacancy clusters are represented by filled and empty triangles, respectively. The inset in (a) represents the detail of the same plot..

to the defects chemical environment. This approach reflects an intuitive idea that the PBE should depend on the chemical environment of the studied defect.

The range of momenta (p) used for the calculation of the W parameter was $15 \times 10^{-3} m_e c < p < 25 \times 10^{-3} m_e c$. The area of the calculated HMPs was normalised to unity. The HMP ratio curves with respect to Ag bulk for the selected defects are shown in Fig. 3. The essential positron characteristics (PLs, PBEs and W parameters) for these defects are plotted in Fig. 4 together with the corresponding parameters for vacancy clusters in fcc Ag and Co.

As shown in Fig. 3 the HMP ratio curve of Co bulk exhibits a well-defined peak at momentum $p \approx 24 \times 10^{-3} m_e c$ and an increase at momenta $p > 40 \times 10^{-3} m_e c$. These features enable to identify the presence of Co atoms surrounding a positron annihilation site. Presence of additional open volume at an annihilation site is seen as a lowering of the ratio curves compared to that for bulk at momenta $p > 10 \times 10^{-3} m_e c$.

The ratio curve for the defect A1, which has size ≈ 0.4 Ag vacancy, lies between the curves for bulk and monovacancy in fcc Ag. In a similar manner, the ratio curve for the defect A2 with size ≈ 2.3 Ag vacancy lies between the curves for a di-vacancy and triple-vacancy in fcc Ag. The presence of Co could not be seen in these ratio curves. Indeed, the W_1/W values (Table) show that only 1% of the Co core electrons participated on annihilation. PLs, PBEs, and the W parameters for the defects A1 and A2 are in good agreement with the reference curve calculated for vacancy clusters in fcc Ag (see Fig. 4).

The ratio curve for the defect C1, which has size ≈ 0.7 Co vacancy, follows the ratio curve of Co monovacancy. This is because the positron trapping occurs not only at the FV but to some extent at the interface between two Co clusters where this defect is located. PL and W parameter would fit better to the reference curve for Co vacancy clusters if the size of C1 were slightly increased (see Fig. 4). However, it should be mentioned that for FV smaller than a monovacancy the reference curve could be only a very rough estimation.

In the case of the defect C2, trapping occurs in the two FVs separated from each other at the distance ≈ 5.7 Å. Both the FVs have the size ≈ 0.7 Co vacancy. There are no Ag atoms surrounding these FVs in the nearest neighbour positions, but there are some Ag atoms at positions of the second and third neighbours. The ratio curve for the defect C2 lies below the ratio curve for Co triple-vacancy (see Fig. 3) mainly due to annihilations with Ag core electrons ($W_1/W = 0.13$). The defect C2 is represented by two points in Fig. 4: first (empty square) corresponds to the size of a single defect, while the second (crossed square) corresponds to the sum of FVs taking part in the positron trapping. The W parameter for the defect C2 lies below the reference curve for defects in pure Co due to annihilations with Ag electrons. Regarding PL and PBE, the reference curve for defects in pure Co lies between these two points considered for the defect C2. The estimated effective size of such defect is ≈ 9–11 Å^3. It shows that in the case of positron localisation at several small FVs, PL increases comparing to that in well-separated FV, but, simultaneously, the size of such composed defect cannot be simply estimated as a sum of the open volumes of defects which take part in the trapping. Similar interaction between FVs occurs also at grain boundaries as shown in Refs. [15, 16]. Understanding how the interaction between defects influences PL and HMP seems to be essential for proper interpretation of the experimental results.

In case of the defect AC1, trapping occurs in the FV on Ag/Co interface surrounded by equal number of Ag and Co nearest neighbour atoms. However, the ratio $W_1/W = 0.64$ indicates that positrons trapped at FV do not necessarily annihilate with electrons belonging to the nearest neighbour atoms only, but they are able to "scan" the chemical environment further. To some extent this is the case of all studied defects. As shown in Table the fraction N_1/N which represents a fraction of the nearest neighbour Ag atoms of defects slightly differs from W_1/W which is a fraction of Ag core electrons taking part in the annihilation process. As

shown in Fig. 3 the ratio curve for the defect AC1 exhibits a peak at momentum $p \approx 24 \times 10^{-3} m_e c$ but no increase at momenta $p > 40 \times 10^{-3} m_e c$. As shown in Fig. 4, PL, PBE and W parameter for the defect AC1 lies between the values for the defects A1 and C1, i.e. defects approximately of the same size in Ag and Co environments, respectively. It shows that these positron characteristics are sensitive to chemical environment of the defects and positron annihilation spectroscopy can be, therefore, a suitable tool for studying defects in AgCo nanocrystalline materials.

5. Conclusions

Analyses of open volume defects in an AgCo nanowire during isothermal and isoenergetic deformation show that the most FVs are small and located predominantly in Ag. There is a correlation between the size and the chemical environment of the defects. The largest defects are located in Ag and the size of FVs decreases with the increasing Co content around the defect. Mechanical strain causes no evolution of FVs. All changes found in the studied sample are induced by the temperature raise. The FV concentration was found to be much higher than the equilibrium vacancy concentration. This is due to a non-crystalline state of Ag. The Co cluster coalescence can be probably related to the increasing number of defects located at the Ag/Co interface.

Simulations of the positron response show that all calculated positron characteristics are sensitive to the chemical environment and the size of the defects. The HMP ratio curve of Co bulk to Ag bulk exhibits a well-defined peak at the momentum $p \approx 24 \times 10^{-3} m_e c$ and an increase at momenta $p > 40 \times 10^{-3} m_e c$, which allows to clearly distinguish the presence of Co atoms around positron annihilation sites. A defect located in Co environment represents a deeper positron trap and results in a higher positron lifetime compared to a defect of the same size in Ag. On the other hand, there is an essential difference of positron affinities of Ag and Co, which causes that the preferential place for positron annihilation is Ag. Positron localisation in separated but closely spaced FVs was observed and the corresponding positron lifetime is prolonged compared with the positron lifetime in the single FV. Simulations also show that positrons are sensitive not only to nearest neighbours of a defect, but they are also able to "scan" chemical environment beyond the nearest neighbour atoms. Considerations concerning possible interaction among defects and not complete positron localisation inside defects seem to be essential for proper interpretation of experimental results. In general, positron annihilation spectroscopy appears to be a suitable tool for studying defects in AgCo nanocrystalline materials.

Acknowledgments

We are grateful to M.J. Puska for his ATSUP code that served as a basis for further developments. O.M. is thankful for a grant of the Université Libre de

Bruxelles and of the Fonds National de la Recherche Scientifique of Belgium, under agreement 2.4520.03F. S.P. is grateful to the Science Policy Office of the Federal Government of Belgium for a grant in the frame of the IAP 5-1 project "Quantum size effects in nanostructured materials". This work is part of the research plan MS 0021620834 and the project COST OC165 supported by the Ministry of Education of the Czech Republic. The presented research is also carried out within the framework of the COST Action P19 "Multiscale Modelling of Materials". This research is supported by the Grant Agency of the Czech Republic (project No. 202/06/1509).

References

[1] E.E. Zhurkin, T. Van Hoof, M. Hou, *Phys. Rev. B* **75**, 224102 (2007).

[2] S.M. Foiles, M.I. Baskes, M.S. Daw, *Phys. Rev. B* **33**, 7983 (1986).

[3] R.A. Johnson, *Phys. Rev. B* **41**, 9717 (1990).

[4] S. Pisov, O. Melikhova, M. Hou, *CCP 2007, Brussels*, accepted for publication in Computational Physics Communications.

[5] J. Kuriplach, *Appl. Surf. Sci.* **194**, 61 (2002).

[6] J. Kuriplach, S. van Petegem, M. Hou, E.E. Zhurkin, H. van Swygenhoven, F. Dalla Torre, G. van Tendeloo, M. Yandouzi, D. Schryvers, D. Segers, A.L. Morales, S. Ettaoussi, C. Dauwe, *Mater. Sci. Forum* **363-365**, 94 (2001).

[7] J. Kuriplach, *Acta Phys. Pol. A* **107**, 784 (2005).

[8] M.J. Puska, R.M. Nieminen, *J. Phys. F, Met. Phys.* **13**, 333 (1983).

[9] A.P. Seitsonen, M.J. Puska, R.M. Nieminen, *Phys. Rev. B* **51**, 14057 (1995).

[10] E. Boroński, R.M. Nieminen, *Phys. Rev. B* **34**, 3820 (1986).

[11] J. Kuriplach, A.L. Morales, C. Dauwe, D. Segers, M. Sob, *Phys. Rev. B* **58**, 10475 (1998).

[12] J.J. Burton, *Phys. Rev. B* **5**, 2948 (1972).

[13] K. Mosig, J. Wolff, J.E. Kluin, T. Hehenkamp, *J. Phys., Condens. Matter* **4**, 1447 (1992).

[14] M.J. Puska, R.M. Nieminen, *Rev. Mod. Phys.* **66**, 841 (1994).

[15] J. Kuriplach, O. Melikhova, M. Hou, S. Van Petegem, E. Zhurkin, M. Šob, *Phys. Status Solidi C* **4**, 3461 (2007).

[16] J. Kuriplach, O. Melikhova, M. Hou, S. Van Petegem, E. Zhurkin, M. Šob, submitted to *Appl. Surf. Sci.*